Ancient viral genomes reveal introduction of HBV and B19V into Mexico during the transatlantic slave trade.

Axel A. Guzmán-Solís[1,2]*, Daniel Blanco-Melo[3]*‡, Viridiana Villa-Islas[1], Miriam J. Bravo-López[1], Marcela Sandoval-Velasco[4], Julie K. Wesp[5], Jorge A. Gómez-Valdés[6], María de la Luz Moreno-Cabrera[7], Alejandro Meraz-Moreno[7], Gabriela Solís-Pichardo[8], Peter Schaaf[9], Benjamin R. tenOever[3] & María C. Ávila-Arcos[1]‡.

1.International Laboratory for Human Genome Research, Universidad Nacional Autónoma de México (México); 2.Aaron Diamond AIDS Research Center, Columbia University Vagelos College of Physicians and Surgeons (NY, USA); 3.Department of Microbiology, Icahn School of Medicine at Mount Sinai (NY, USA); 4.Section for Evolutionary Genomics, The Globe Institute, Faculty of Health, University of Copenhagen (Denmark); 5.Department of Sociology and Anthropology, North Carolina State University (USA); 6.Escuela Nacional de Antropología e Historia (México); 7.Instituto Nacional de Antropología e Historia (México); 8.Laboratorio Universitario de Geoquímica Isotópica (LUGIS), Instituto de Geología, Universidad Nacional Autónoma de México (México); 9.LUGIS, Instituto de Geofísica, Universidad Nacional Autónoma de México (México).

* These authors contributed equally to this work. ‡ Correspondence: daniel.blancomelo@mssm.edu (D.B-M.), mavila@liigh.unam.mx (M.C.A-A.).

ABSTRACT

After the European colonization of the Americas there was a dramatic population collapse of the Indigenous inhabitants caused in part by the introduction of new pathogens. Although there is much speculation on the etiology of the Colonial epidemics, direct evidence for the presence of specific viruses during the Colonial era is lacking. To uncover the diversity of viral pathogens during this period, we designed an enrichment assay targeting ancient DNA (aDNA) from viruses of clinical importance and applied it on DNA extracts from individuals found in a Colonial hospital and a Colonial chapel (16^{th} c. – 18^{th} c.) where records suggest victims of epidemics were buried during important outbreaks in Mexico City. This allowed us to reconstruct three ancient human parvovirus B19 genomes, and one ancient human hepatitis B virus genome from distinct individuals. The viral genomes are similar to African strains, consistent with the inferred morphological and genetic African ancestry of the hosts as well as with the isotopic analysis of the human remains, suggesting an origin on the African continent. This study provides direct molecular evidence of ancient viruses being transported to the Americas during the transatlantic slave trade and their subsequent introduction to New Spain. Altogether, our observations enrich the discussion about the etiology of infectious diseases during the Colonial period in Mexico.

INTRODUCTION

European colonization in the Americas resulted in a frequent genetic exchange mainly between Native American populations, Europeans, and Africans (Aguirre-Beltrán, 2005; Rotimi et al., 2016; Salas et al., 2004). Along with human migrations, numerous new species were introduced to the Americas including bacterial and viral pathogens, which played a major role in the dramatic population collapse that afflicted the immunologically-naïve Indigenous inhabitants (Acuña-Soto et al., 2004; Lindo et al., 2016). Among these pathogens, viral diseases, such as smallpox, measles and mumps have been proposed to be responsible for many of the devastating epidemics during the Colonial period (Acuña-Soto et al., 2004). Remarkably, the pathogen(s) responsible for the deadliest epidemics reported in New Spain (the Spanish viceroyalty that corresponds to Mexico, Central America, and the current US southwest states) remains unknown and is thought to have caused millions of deaths during the 16th century[4]. Indigenous populations were drastically affected by these mysterious epidemics, generically referred to as *Cocoliztli* ("pest" in Nahuatl)[6], followed by Africans and to a lesser extent European people (Acuña-Soto et al., 2004; Malvido & Viesca, 1982; Somolinos d'Árdois, 1982). Symptoms of the 1576 *Cocoliztli* epidemic were described in autopsy reports of victims treated at the "Hospital Real de San José de los Naturales" (HSJN) (Malvido & Viesca, 1982; Wesp, 2017), the first hospital in Mexico dedicated specifically to treat the Indigenous population (Malvido & Viesca, 1982; Wesp, 2017) (Figure 1a-b). The symptoms described included high fever, severe headache, neurological disorders, internal and external bleeding, hepatitis and intense jaundice (Acuña-Soto et al., 2004; Malvido & Viesca, 1982; Somolinos d'Árdois, 1982). This has led some

scholars to postulate that the etiological agent of the *Cocoliztli* epidemic was a hemorrhagic fever virus (Acuña-Soto et al., 2004; Marr & Kiracofe, 2000), although others have suggested that the symptoms could be explained by bacterial infections (Malvido & Viesca, 1982; Vågene et al., 2018).

The study of ancient viral genomes has revealed important insights into the evolution of specific viral families (Barquera et al., 2020; Duggan et al., 2016; Düx et al., 2020; Kahila Bar-Gal et al., 2012; Krause-Kyora et al., 2018, p.; Mühlemann, Jones, et al., 2018, 2018; Mühlemann, Margaryan, et al., 2018; Neukamm et al., 2020; Pajer et al., 2017; Patterson Ross et al., 2018; Xiao et al., 2013), as well as their interaction with human populations (Spyrou et al., 2019). To explore the presence of viral pathogens in circulation during epidemic periods in New Spain, we leveraged the vast historical and archeological information available for the Colonial HSJN. These include the skeletal remains of over 600 individuals recovered from mass burials associated with the hospital's architectural remnants (Figure 1b). Many of these remains were retrieved from burial contexts suggestive of an urgent and simultaneous disposal of the bodies, as in the case of an epidemic (Meza, 2013; Wesp, 2017). Prior bioarcheological research has shown that the remains of a number of individuals in the HSJN collection displayed dental modifications and/or morphological indicators typical of African ancestry (Meza, 2013), consistent with historical and archeological research that documents the presence of a large number of both free and enslaved Africans and their descendants in Colonial Mexico (Aguirre-Beltrán, 2005). Indeed a recent paleogenomics study reported a Sub-Saharan African origin of three individuals from this collection (Barquera et al., 2020).

Here we describe the recovery and characterization of viral pathogens that circulated in New Spain during Colonial times, using ancient DNA (aDNA) techniques (Supplementary Figure 1). For this work, we sampled skeletal human remains recovered from the HSJN where archeological context suggest victims of epidemics were buried (Meza, 2013) and from “La Concepcion” chapel, one of the first catholic conversion centers in New Spain (Moreno-Cabrera et al., 2015) (Figure 1a). We report the reconstruction of ancient hepatitis B virus (HBV) and human parvovirus B19 (B19V) genomes recovered from these remains. Our findings provide a direct molecular evidence of human viral pathogens of African origin being introduced to New Spain during the transatlantic slave trade.

RESULTS

We sampled the skeletal remains from two archeological sites, a Colonial Hospital and a Colonial chapel in Mexico City (Figure 1a-b). For the HSJN, 21 dental samples (premolar and molar teeth) were selected based on previous morphometric analyses and dental modifications that suggested an African ancestry (Hernández-Lopez & Negrete, 2012; Karam-Tapia, 2012; Meza, 2013; Ruíz-Albarrán, 2012). The African presence in the Indigenous Hospital might reflect an urgent response to an epidemic outbreak, since hospitals treated patients regardless of the origin of the affected individuals during serious public health crises (Meza, 2013). Dental samples of five additional individuals were selected (based on their conservation state) from “La Concepción” chapel (COY), which is located 10 km south of the HSJN in Coyoacán, a Pre-Hispanic Indigenous neighborhood that became the first Spanish settlement

121 in Mexico City after the fall of Tenochtitlan (Moreno-Cabrera et al., 2015). Following
122 strict aDNA protocols, we processed these dental samples to isolate aDNA for next-
123 generation sequencing (NGS) (Supplementary Figure 1, Methods). Teeth roots
124 (which are vascularized) can be a good source of pathogen DNA(Key et al., 2017),
125 especially in the case of viruses that are widespread in the bloodstream during
126 systemic infection. Accordingly, a number of previous studies have successfully
127 recovered ancient viral DNA from teeth roots (Barquera et al., 2020; Krause-Kyora
128 et al., 2018; Mühlemann, Jones, et al., 2018; Mühlemann, Margaryan, et al.,
129 2018),(Mühlemann et al., 2020).
130
131 Metagenomic analysis with MALT (Vågene et al., 2018) (Methods) on the NGS data
132 using the Viral NCBI RefSeq database as a reference (Pruitt et al., 2007), revealed
133 seventeen samples contained at least one normalized hit to viral DNA, particularly
134 similar to *Hepadnaviridae*, *Herpesviridae*, *Parvoviridae* and *Poxviridae* (Figure 1c,
135 Supplementary Figure 2a, Methods). These viral hits revealed the potential to
136 recover ancient viral genomes from these samples. We selected twelve samples for
137 further screening (Figure 1c, Supplementary Figure 2b) based on the DNA
138 concentration of the NGS library and the quality of the hits to a clinically important
139 virus (HBV, B19V, Papillomavirus, Smallpox). To isolate and enrich the viral DNA
140 fraction in the sequencing libraries, biotinylated single-stranded RNA probes
141 designed to capture sequences from diverse human viral pathogens were
142 synthesized (Supplementary Table 1). The selection of the viruses included in the
143 capture design considered the following criteria: 1) DNA viruses previously retrieved
144 from archeological human remains (i.e. Hepatitis B virus, Human Parvovirus B19,

Variola Virus), 2) representative viruses from families capable of integrating into the human genome (i.e. *Herpesviridae*, *Papillomaviridae*, *Polyomaviridae*, *Circoviridae*) or 3) RNA viruses with a DNA intermediate (i.e. *Retroviridae*). Additionally, a virus-negative aDNA library, which showed no hits to any viral family included in the capture assay (except for a frequent *Poxviridae*-like region identified as an Alu repeat (Tithi et al., 2018)), was captured and sequenced as a negative control (HSJN177) to estimate the efficiency of our capture assay. Four post-capture libraries had a ~100-fold increase of HBV-like hits or a ~50-200-fold increase of B19V-like hits (Figure 1c, Supplementary Table 2) compared to their corresponding pre-capture libraries (Methods). In contrast, the captured negative control (HSJN177) presented a negligible enrichment of these viral hits (Figure 1c, Supplementary Table 2).

We verified the authenticity of the viral sequences by querying the mapped reads against the non-redundant (nr) NCBI database using megaBLAST(Altschul et al., 1990). We only retained reads for which the top hit was to either B19V or HBV, respectively (Supplementary Table 3). 1 To confirm the ancient origin of these viral reads, we evaluated the misincorporation damage patterns using the program mapDamage 2.0 (Jónsson et al., 2013), which revealed an accumulation of C to T mutations towards their 5' terminal site with an almost symmetrical G to A pattern on the 3' end (Figure 2a, Supplementary Figure 3a), as expected for aDNA (Briggs et al., 2007). Three ancient B19V genomes were reconstructed (Figure 2b, Supplementary Table 3) with sequence coverages between 92.37% and 99.1%, and average depths of 2.98-15.36X along their single stranded DNA (ssDNA) coding

region, which excludes the double stranded DNA (dsDNA) hairpin regions at each end of the genome (Luo & Qiu, 2015). These dsDNA inverse terminal repeats (ITRs) displayed considerably higher depth values (<218X) compared to the coding region consistent with the better *post-mortem* preservation of dsDNA compared to ssDNA (Lindahl, 1993) (Figure 2b). In addition, we reconstructed one ancient HBV genome (Figure 2c, Supplementary Table 3) at 30.8X average depth and with a sequence coverage of 89.9%, including its ssDNA region at a reduced depth (<10X). This genome shows a 6 nucleotide (nt) insertion in the core gene, which is characteristic of the genotype A (Kramvis, 2014). Further phylogenetic analyses (Methods) revealed that the Colonial HBV genome clustered with modern sequences corresponding to sub-genotype A4 (previously named A6) (Pourkarim et al., 2014) (Figure 3a, Supplementary Figure 4). The Genotype A (HBV/GtA) has a broad diversity in Africa reflecting its long history in this continent (Kostaki et al., 2018; Kramvis, 2014), while the sub-genotype A4 has been recovered uniquely from African individuals in Belgium (Pourkarim et al., 2010) and has never been found in the Americas. Regarding the three Colonial B19V genomes from individuals HSJN240, COYC4 and HSJNC81, these were phylogenetically closer to modern B19V sequences belonging to genotype 3 (Figure 3b, Supplementary Figure 5a-b). This B19V genotype is divided into two sub-genotypes: 3a that is mostly found in Africa, and 3b, which is proposed to have spread outside Africa in the last decades (Hübschen et al., 2009). The viral sequences from the individuals HSJN240 and COYC4 are similar to sub-genotype 3b genomes sampled from immigrants (Morocco, Egypt and Turkey) in Germany (Schneider et al., 2008) (Figure 3b, Supplementary Figure 5a-b); while the sequence of the individual HSJNC81 is more

similar to a divergent sub-genotype 3a strain (Figure 3b, Supplementary Figure 5a-b) retrieved from a child with severe anemia born in France (Nguyen et al., 1999). These observations support the African origin of the reconstructed colonial viral genomes.

In order to infer the temporal dynamics between our samples and the rest of the viral diversity, we first estimated if the phylogenetic relationships among B19V or HBV genomes had a temporal structure. Similarly to previous studies (Krause-Kyora et al., 2018), we found little or no temporal structure for this HBV phylogeny containing all genotypes (R^2=0.1351; correlation coefficient=0.3676) (Supplementary Figure 6a-c). The complex evolution of HBV may not be prone to an appropriate genetic dating since multiple recombination and cross-species transmission (Human-Ape) events (Krause-Kyora et al., 2018) occurred throughout its evolution. Since the entire Genotype A has been identified as a recombinant genotype before (Mühlemann, Jones, et al., 2018) we analyzed it independently and identified a stronger temporal signal within this genotype (R^2=0.722; correlation coefficient=0.8498) (Supplementary Figure 6d-f). In the case of B19V we identified a temporal structure when including all three genotypes (R^2=0.3837; correlation coefficient=0.6194) (Supplementary Figure 7a-c), in agreement with previous studies (Mühlemann, Margaryan, et al., 2018). Furthermore, we corroborated this temporal structure was not an artifact by a set of tip-dated randomized analyses (Rieux & Balloux, 2016), where none of clock rate 95% highest posterior density (HPD) intervals overlapped with the correctly dated dataset (Supplementary Figure 8).

With these results we then performed a dated coalescent phylogenetic analysis. We inferred a median substitution rate for B19V of 1.03×10^{-5} (95% HPD: 8.66×10^{-6}-1.21×10^{-5}) s/s/y under a strict clock and a constant population prior and a substitution rate of 2.62×10^{-5} (95% HPD: 1.50×10^{-5}-3.98×10^{-5}) s/s/y under a relaxed log normal clock and a constant population prior. The divergence times from the most recent common ancestor of genotypes 1, 2 and 3 under a strict clock were 7.19 (95% HPD: 6.98-7.46), 2.11 (95% HPD: 1.83-2.51), and 3.64 (95% HPD: 3.04-4.33) ka, respectively. The inferred substitution rates and divergence times from the most recent common ancestor for genotypes 1 and 2 were similar to previous estimations (Mühlemann, Margaryan, et al., 2018) that included much older sequences, while the divergence of genotype 3 was subtly older since no other ancient genotype 3 had been reported previously.

Next, we used the *de novo* generated sequence data to determine the mitochondrial haplogroup of the hosts, as well as their autosomal genetic ancestry using the 1000 Genomes Project (1000 Genomes Project Consortium et al., 2015) as a reference panel (Figure 4a, Supplementary Table 4). The nuclear genetic ancestry analysis showed that all three HSJN individuals, from which the reconstructed viral genomes were isolated, fall within African genetic variation in a Principal Component Analysis plot (Figure 4a), while their mitochondrial aDNA belong to the L haplogroup, which has high frequency in African populations (Supplementary Table 4, Supplementary Figure 3b). Additionally, we performed $^{87}Sr/^{86}Sr$ isotopic analysis on two of the HSJN individuals using teeth enamel as well as phalange (HSJN240) or parietal bone (HSJNC81) to provide insights on the places of birth (adult enamel) and where the

last years of life were spent (phalange/parietal). The $^{87}Sr/^{86}Sr$ ratios measured on the enamel of the individual HSJNC81 (0.71098) and HSJN240 (0.71109) are similar to average $^{87}Sr/^{86}Sr$ ratios found in soils and rocks from West Africa (average of 0.71044, Supplementary Figure 9, Supplementary Tables 6 and 7), as well as to $^{87}Sr/^{86}Sr$ ratios described in first generation Africans in the Americas (Barquera et al., 2020; Bastos et al., 2016; Fricke et al., 2020; T. D. Price et al., 2012; Schroeder et al., 2009). In contrast, the $^{87}Sr/^{86}Sr$ ratios on the parietal and phalange bones from the HSJNC81 (0.70672) and HSJN240 (0.70755), show lower values similar to those observed in the Trans Mexican Volcanic Belt where the Mexico City Valley is located (0.70420 - 0.70550, Supplementary Figure 9, Supplementary Tables 6 and 7). Moreover, radiocarbon dating of HSJN240 (1442-1608 CE, years calibrated for 1σ) and HSJN194 (1472-1625 CE, years calibrated for 1σ) (Supplementary Table 4, Supplementary Figure 10) indicates that these individuals arrived during the first decades of the Colonial period, when the number of enslaved individuals arriving from Africa was particularly high (Aguirre-Beltrán, 2005). Strikingly, Colonial individual COYC4, who was also infected with an African B19V strain, clusters with present-day Mexicans and Peruvians from the 1000 Genomes Project (Figure 4a). An ADMIXTURE (Alexander & Lange, 2011) analysis with these data confirmed a predominant Native American and African genetic component (Figure 4b), as expected for a post-contact individual. The B19V ancient genome from the individual COYC4 is the first genotype 3 genome obtained from a non-African individual and suggests that following the introduction from Africa, the virus (B19V) spread and infected people of different ancestries during Colonial times.

DISCUSSION

In this study we reconstructed one HBV and three B19V ancient genomes from four different individuals using NGS, metagenomics and in-solution targeted enrichment methods (Figure 2b, c, Supplementary Figure 1). Several lines of evidence support the ancient nature of these viral sequences, in contrast to environmental contamination or a capture artifact. First, our negative control was not enriched for B19V or HBV hits in our capture sequencing (Figure 1c). For those samples that showed an enrichment in viral sequences after capture, the reads covered the reference genomes almost in their entirety and displayed deamination patterns at the terminal ends of the reads, as expected for aDNA (Figure 2a). Moreover, it is important to notice that B19V and HBV are blood-borne human pathogens that are not present in soil or the environment, and that DNA from these viruses had never been extracted before in the aDNA facilities used for this study.

We also described an unusual coverage pattern on the B19V genome, where the dsDNA hairpins at its terminal sites are highly covered reflecting a better stability of these regions over time (Figure 2b). Similarly, the partially circular dsDNA genome from HBV was poorly covered at the ssDNA region (Figure 2c), as found in three previously reported ancient HBV genomes (Krause-Kyora et al., 2018) (Supplementary Discussion 1). The variable read coverage in both viruses argues against an integration event of these viruses, which would result in a uniform dsDNA coverage; further analyses are needed to determine if the aDNA retrieved in this and other studies comes from systemic circulating virions or from systemic cell-free DNA

287 intermediates (Cheng et al., 2019) produced after viral replication in the bone marrow
288 or liver, for B19V and HBV, respectively (Broliden et al., 2006; Yuen et al., 2018).
289
290 The ancient B19V genomes were assigned to genotype 3. This genotype is the most
291 prevalent in West Africa (Ghana: 100%, n=11; Burkina Faso: 100%, n=5) (Candotti
292 et al., 2004; Hübschen et al., 2009; Rinckel et al., 2009) and a potential African origin
293 has been suggested (Candotti et al., 2004). It has also been sporadically found
294 outside Africa (Jain et al., 2015),(Candotti et al., 2004; Rinckel et al., 2009) in
295 countries historically tied to this continent, like Brazil (50%, n=12) (Freitas et al.,
296 2008; Sanabani et al., 2006), India (15.4%, n=13) (Jain et al., 2015), France (11.4%,
297 n=79) (Nguyen et al., 1999; Servant et al., 2002), and USA (0.85%, n=117) (Rinckel
298 et al., 2009) as well as in immigrants from Morocco, Egypt, and Turkey in Germany
299 (6.7%, n=59) (Schneider et al., 2008). Two other genotypes, 1 and 2 exist for this
300 virus. Genotype 1 is the most common and is found worldwide, while the almost
301 extinct genotype 2 is mainly found in elderly people from Northern Europe (Pyöriä et
302 al., 2017). Ancient genomes from genotypes 1 and 2 have been recovered from
303 Eurasian samples, including a genotype 2 B19V genome from a 10th century Viking
304 burial in Greenland (Mühlemann, Margaryan, et al., 2018). $^{87}Sr/^{86}Sr$ isotopes on
305 individuals from such burial revealed they were immigrants from Iceland
306 (Mühlemann, Margaryan, et al., 2018), suggesting an introduction of the genotype 2
307 to North America during Viking explorations of Greenland.
308
309 While serological evidence indicates that B19V currently circulates in Mexico, only
310 the presence of genotype 1 has been formally described using molecular analyses

(Valencia Pacheco et al., 2017). Taken together, our results are consistent with an introduction of the genotype 3 to New Spain as a consequence of the transatlantic slave trade imposed by the European colonization. This hypothesis is supported by the $^{87}Sr/^{86}Sr$ isotopic analysis, which gives evidence that the individuals from the HSJN with B19V (HSJN240, HSJNC81) were born in West Africa and spent their last years of life in New Spain (Supplementary Figure 9). Furthermore, the radiocarbon ages of individuals HSJN240, HSJN194 (Supplementary Figure 10) support this notion as they correspond to the Early Colonial period, during which the number of enslaved Africans arriving was higher compared to later periods (Aguirre-Beltrán, 2005). Remarkably, a B19V genome belonging to the genotype 3 was recovered from an admixed individual (COYC4) (Figure 4b) with a predominant Indigenous ancestry as well as some African. COY4 was excavated in an independent archeological site 10 Km south of the HSJN (Figure 1a), supporting the notion that viral transmissions between African individuals and people of different ancestries occurred during the Colonial period in Mexico City.

The genotype A from HBV is highly diverse in Africa, reflecting its long evolutionary history, and likely originated somewhere between Africa, Middle East and Central Asia (Kostaki et al., 2018). The introduction of the genotype A from Africa to the Americas has been proposed based on phylogenetic analysis of modern strains from Brazil (Freitas et al., 2008; Kostaki et al., 2018) and Mexico (Roman et al., 2010), and more precisely to the sub-genotype A1 using sequences from Martinique (Brichler et al., 2013), Venezuela (Quintero et al., 2002), Haiti (Andernach et al., 2009), and Colombia (Alvarado-Mora et al., 2012). Recently, a similar introduction

335 pattern was proposed for the quasi genotype A3 based on an ancient HBV genome
336 recovered from an ancient African individual sampled in Mexico (Barquera et al.,
337 2020). The origin of the sub-genotype 4 is controversial with an apparent African
338 origin based on sequences recovered from African individuals in Europe (Pourkarim
339 et al., 2010). The Colonial ancient HBV genome reconstructed in our work is
340 assigned to genotype A4 (Figure 3a, Supplementary Figure 4), which represents the
341 first report of this sub-genotype in the Americas and further supports its African
342 origin. The introduction of the pathogens from Africa to the Americas has been
343 proposed for other human-infecting viruses such as smallpox (Mandujano-Sánchez
344 et al., 1982; Somolinos d'Árdois, 1982), based on historical records; or Yellow fever
345 virus (Bryant et al., 2007), HTLMV-1 (Gadelha et al., 2014), Hepatitis C virus
346 (genotype 2) (Markov et al., 2009) and human herpes simplex virus (Forni et al.,
347 2020) based on phylogenetic analysis of modern strains from Afro-descendant or
348 admixed human populations.
349
350 Although we cannot assert where exactly the African-born individuals in this study
351 contracted B19V or HBV (Africa, America, or the Middle Passage) nor if the cause
352 of their deaths can be attributed to such infections, the identification of ancient B19V
353 and HBV in contexts associated with Colonial epidemics in Mexico City is still
354 relevant in light of their paleopathological marks and the clinical information available
355 for the closest sequences in the phylogenetic analyses. The reconstructed ancient
356 B19V genome from individual HSJNC81 is closest to the V9 strain, which was
357 isolated from an individual with severe anemia(Nguyen et al., 1999) (AJ249437)
358 (Figure 3b). Noteworthy, individual HSJNC81 displayed cribra orbitalia in the eye

359 sockets and porotic hyperostosis on the cranial vault (Supplementary Figure 11),
360 morphological changes typically associated with anemias of varying different causes
361 (Angel, 1966). It is acknowledged that B19V infection can cause severe or even fatal
362 anemia due to the low level of hemoglobin when present simultaneously with other
363 blood disorders, as thalassemia, sickle-cell anemia, malaria and iron deficiency
364 (Broliden et al., 2006; Heegaard & Brown, 2002). Therefore, since B19V infects
365 precursors of the erythroid lineage (Broliden et al., 2006), it is possible that the
366 morphological changes found in HSJNC81 might be the result of a severe anemia
367 caused or enhanced by a B19V infection (Supplementary Discussion 2). Moreover,
368 the identification of ancient B19V in a Colonial context is noteworthy considering
369 several recent reports that reveal that measles-like cases were actually attributable
370 to B19V (De Los Ángeles Ribas et al., 2019; Rezaei et al., 2016). Therefore it is
371 possible that B19V might have been responsible for some of the numerous cases of
372 measles that were described in early 16th century Mexico (Acuña-Soto et al., 2004;
373 Mandujano-Sánchez et al., 1982; Wesp, 2017), as well as in historical records that
374 account for the treatment of an outbreak of measles at the HSJN in 1531 (Meza,
375 2013) (Supplementary Discussion 2). Nevertheless, this hypothesis requires
376 additional comprehensive studies aimed to characterize the presence of measles
377 and rubella viruses from ancient remains, a task that imposes difficult technical
378 challenges given that RNA is known to degrade rapidly. In fact most ancient viral
379 RNA genomes have been recovered only from formalin-fixed tissue (Düx et al., 2020;
380 Xiao et al., 2013)
381

382 Furthermore, historical records of the autopsies of victims of the 1576 *Cocoliztli*
383 epidemic treated at the HSJN, describe the observation of enlarged hard liver and
384 jaundice (Acuña-Soto et al., 2002, 2004; Malvido & Viesca, 1982; Marr & Kiracofe,
385 2000; Somolinos d'Árdois, 1982), which could be explained by severe liver damage
386 or epidemic hepatitis (Acuña-Soto et al., 2004; Malvido & Viesca, 1982). This is
387 noteworthy given both viruses HBV and B19V proliferate in the liver and are
388 associated to hepatitis and jaundice (Broliden et al., 2006; Yuen et al., 2018).
389 However, it is important to acknowledge that both viruses have also been previously
390 identified in aDNA datasets not necessarily associated with disease or epidemic
391 contexts (Kahila Bar-Gal et al., 2012; Krause-Kyora et al., 2018; Mühlemann, Jones,
392 et al., 2018; Patterson Ross et al., 2018), thus establishing a direct link would require
393 additional samples and a more comprehensive pathogen screening to rule out the
394 involvement of other pathogens. Finally, although our data does not provide
395 conclusive evidence of the involvement of HBV and B19V in the reported
396 manifestations of liver damage in *Cocoliztli* autopsies, the identification of these
397 viruses in likely victims of epidemic outbreaks in the Colonial period opens up new
398 opportunities for investigating the presence of these viruses in similar contexts. This
399 type of research is particularly relevant when considering previous hypotheses
400 favoring the synergistic action of different types of pathogens in these devastating
401 Colonial epidemics (Somolinos d'Árdois, 1982) (Supplementary Discussion 3).
402
403 It is important to emphasize that our findings should be interpreted with careful
404 consideration of the historical and social context of the transatlantic slave trade. This
405 cruel episode in history involved the forced displacement of millions of individuals to

406 the Americas (ca. 250,000 to New Spain (Aguirre-Beltrán, 2005)) under inhumane,
407 unsanitary and overcrowded conditions that, with no doubt, favored the spread of
408 infectious diseases (Mandujano-Sánchez et al., 1982). Therefore, the introduction of
409 these and other pathogens from Africa to the Americas should be attributed to the
410 brutal and harsh conditions of the Middle passage that enslaved Africans were
411 subjected to by traders and colonizers, and not to the African peoples themselves.
412 Moreover, the adverse life conditions for enslaved Africans and Native Americans,
413 especially during the first decades after colonization, surely favored the spread of
414 diseases and emergence of epidemics (Mandujano-Sánchez et al., 1982).
415 Integrative and multidisciplinary approaches are thus needed to understand this
416 phenomenon at its full spectrum.
417
418 In summary, our study provides direct aDNA evidence of HBV and B19V introduced
419 to the Americas from Africa during the transatlantic slave trade. The isolation and
420 characterization of these ancient HBV and B19V genomes represent an important
421 contribution to the only ancient viral genome recently reported in the Americas
422 (Barquera et al., 2020). Our results expand our knowledge on the viral agents that
423 were in circulation during Colonial epidemics like *Cocoliztli*, some of which resulted
424 in the catastrophic collapse of the immunologically-naïve Indigenous population.
425 Although we cannot assign a direct causality link between HBV and B19V and
426 *Cocoliztli*, our findings confirm that these potentially harmful viruses were indeed
427 circulating in individuals found in archeological contexts associated with this
428 epidemic outbreak. Further analyses from different sites and samples will help
429 understand the possible role of these and other pathogens in Colonial epidemics, as

well as the full spectrum of pathogens that were introduced to the Americas during European colonization.

METHODS

Sample selection and DNA extraction

Dental samples (premolars and molars) were obtained from twenty-one individuals from the skeletal collection of the HSJN, selected based on their African-related skeletal indicators (Hernández-Lopez & Negrete, 2012; Karam-Tapia, 2012; Meza, 2013; Ruíz-Albarrán, 2012). Five additional samples were taken from “La Concepción” chapel, based on their conservation state. Permits 401.1S.3-2018/1373 and 401.1S.3-2020/1310 to carry out this sampling and aDNA analyses were obtained by the Archeology Council of the National Institute of Anthropology and History (INAH) for the Hospital San Jose de los Naturales and “La Concepción” chapel, respectively.

DNA extraction and NGS library construction

Bone samples were transported to a dedicated ancient DNA clean-room laboratory at the International Laboratory for Human Genome Research (LIIGH-UNAM, Querétaro, Mexico), were DNA extraction and NGS-libraries construction was performed under the guidelines on contamination control for aDNA studies (Warinner et al., 2017). Previously reported aDNA extraction protocols were used for the HSJN (Dabney et al., 2013) and COY (Rohland & Hofreiter, 2007) samples. Double-stranded DNA (dsDNA) indexed (6bp) sequencing libraries were constructed from the DNA extract, as previously reported (Meyer & Kircher, 2010). In order to detect

454 contaminants in reagents or by human manipulation, extraction and library
455 constructions protocols included negative controls (NGS blanks) that were analyzed
456 in parallel with the same methodology. The resulting NGS dsDNA indexed libraries
457 were quantified with a Bioanalyzer 2100 (Agilent) and pooled into equimolar
458 concentrations.
459
460 *NGS sequencing*
461 Pooled libraries were paired-end sequenced on an Illumina NextSeq550 at the
462 "Laboratorio Nacional de Genómica para la Biodiversidad" (LANGEBIO, Irapuato,
463 Mexico), with a Mid-output 2x75 format. The reads obtained (R1 and R2) were
464 merged (>11bp overlap) and trimmed with AdapterRemoval 1.5.4 (Schubert et al.,
465 2016). Overlapping reads (>30 bp in length) were kept and mapped to the human
466 genome (hg19) using BWA 0.7.13 (Heng Li & Durbin, 2009). Mapped reads were
467 used for further human analysis (genetic ancestry, and mitochondrial haplogroup
468 determination), whereas unmapped reads were used for metagenomic analysis and
469 viral genome reconstruction.
470
471 *Metagenomic analyses*
472 The NCBI Viral RefSeq database was downloaded on February 2018; this included
473 7530 viral genomes. MALT 0.4.0 (Vågene et al., 2018) software was used to
474 taxonomically classify the reads using the viral genomes database. The viral
475 database was formatted automatically with malt-build once, and not human
476 (unmapped) reads were aligned with malt-run (85 minimal percent identity). The
477 produced RMA files with viral abundances were normalized based on the smallest

478 sample size (default) and compared to all the samples from the same archeological
479 site with MEGAN 6.8.0 (Huson et al., 2016).
480
481 *Capture-enrichment Assay*
482 Twenty-nine viruses were included in the in-solution enrichment design, the
483 complete list of NCBI IDs is provided in Supplementary methods 5 and
484 Supplementary Table 1. It contained viral genomes previously recovered from
485 archeological remains like B19V, B19V-V9, and HBV (consensus genomes),
486 selected VARV genes, as well as clinically important viral families that are able to
487 integrate into the human genome, have dsDNA genomes, or dsDNA intermediates.
488 The resulting design comprised 19,147 ssRNA 80 nt probes targeting, with a 20 nt
489 interspaced distance, the whole or partial informative regions of eight viral families
490 of clinical relevance (*Poxviridae, Hepadnaviridae, Parvoviridae, Herpesviridae,*
491 *Retroviridae, Papillomaviridae, Polyomaviridae, Circoviridae*). To avoid a
492 simultaneous false-positive DNA enrichment, low complexity regions and human-
493 like (hg38) sequences were removed (*in sillico*). The customized kit was produced
494 by Arbor Biosciences (Ann Arbor, MI, USA). Capture-enrichment was performed on
495 the indexed libraries based on the manufacturer's protocol (version 4) to pull-down
496 aDNA with minimal modifications. Libraries were amplified with 18-20 cycles
497 (Phusion U Hot Start DNA Polymerase by Thermo Fischer Scientific), purified with
498 SPRISelect Magnetic Beads (Beckman Coulter) and quantified with a Bioanalyzer
499 2100 (Agilent). Amplified libraries were then pooled in different concentrations and
500 deep sequenced yielding >1x10^6 non-human reads (Supplementary Table 4) in
501 order to saturate the target viral genome. Reads generated from each enriched

library were analyzed exactly as the shotgun (not-enriched) libraries. Normalized abundances between shotgun and captured libraries were compared in MEGAN 6.8.0 (Huson et al., 2016) to evaluate the efficiency and specificity of the enrichment assay.

Viral datasets

The full list of accession numbers of the following datasets is given in Supplementary Methods 8.

HBV-Dataset-1 (HBV/DS1): comprises 38 HBV genomes from modern A-J human genotypes, 2 well-covered ancient HBV genomes (LT992443, LT992459) and a wholly monkey genome.

HBV-Dataset-2 (HBV/DS2): comprises 593 whole genomes downloaded from the NCBI database in August 2020, that included genomes from A-J genotypes as well as non-human primates HBV genomes (gibbon, gorilla, and chimpanzee), 19 ancient HBV genomes (Barquera et al., 2020; Kahila Bar-Gal et al., 2012; Krause-Kyora et al., 2018, p.; Mühlemann, Jones, et al., 2018; Neukamm et al., 2020; Patterson Ross et al., 2018) and one ancient HBV genome from this study (HSJN194).

B19V-Dataset-1 (B19V/DS1): comprises 13 B19V genomes from human genotypes 1-3 as well as a bovine parvovirus.

B19V-Dataset-2 (B19V/DS2): comprises 109 genomes from 1 to 3 B19V genotypes downloaded from the NCBI database in August 2020, that included the 10 best-covered ancient genomes from genotype 1 and 2 (Mühlemann, Margaryan, et al., 2018) as well as 3 ancient B19V from this study. Since many of the reported

525 genomes in our dataset are not complete, only the whole coding region (CDS) was
526 used.
527
528 *Genome Reconstruction and authenticity*
529 HBV: Non-human reads were simultaneously mapped to HBV/DS1 with BWA (aln
530 algorithm) with seedling disabled (Schubert et al., 2012). The reference sequence
531 with the most hits was used to map uniquely to this reference and generate a BAM
532 alignment without duplicates (Ref: GQ331046), from which damage patterns were
533 determined and damaged sites rescaled using mapDamage 2.0 (Jónsson et al.,
534 2013), the rescaled alignment was used to produce a consensus genome. All the
535 HBV mapped reads were analyzed through megaBLAST (Altschul et al., 1990) using
536 the whole NCBI nr database, in order to verify they were assigned uniquely to HBV
537 (carried out with Krona 2.7 (Ondov et al., 2011)).
538 B19V: The reconstruction of the B19V ancient genome was done as previously
539 reported from archeological skeletal remains (Mühlemann, Margaryan, et al., 2018),
540 but increasing the stringency of some parameters as described next. Non-human
541 reads were mapped against B19V/DS1 with BWA (aln algorithm) with seedling
542 disabled(Schubert et al., 2012), if more than 50% of the genome was covered, the
543 sample was considered positive to B19V. Reads from the B19V-positive libraries
544 were aligned with blastn (-evalue 0.001) to B19V/DS1 in order to recover all the
545 parvovirus-like reads. To avoid local alignments, only hits covering >85% of the read
546 were kept and joined to the B19V mapped reads (from BWA), duplicates were
547 removed. The resulting reads were analyzed with megaBLAST (Altschul et al., 1990)
548 using the whole NCBI nr database to verify the top hit was to B19V (carried out with

549 Krona 2.7 (Ondov et al., 2011)). This pipeline was applied for two independent
550 enrichments assays per sample and the filtered reads from the two capture rounds
551 were joined. The merged datasets per sample were mapped using as a reference
552 file the three known B19V genotypes with GeneiousPrime 2019.0.4 (Kearse et al.,
553 2012) using median/fast sensibility and iterate up to 5 times. The genotype with the
554 longest covered sequence was selected as the reference for further analysis (Ref:
555 AB550331). Deamination patterns for HBV and B19V were determined with
556 mapDamage 2.0 (Jónsson et al., 2013) and damaged sites were rescaled in the
557 same program to produce a consensus whole genome using SAMtools 1.9 (H. Li et
558 al., 2009).
559
560 *Phylogenetic analyses*
561 HBV/DS2 and B19V/DS2 were aligned independently in Aliview (Larsson, 2014)
562 (Muscle algorithm), and evolutionary models were tested under an AICc and BIC in
563 jModelTest (Darriba et al., 2012). A neighbor joining tree with 1000 bootstraps was
564 generated in MEGA (Kumar et al., 2018) using a number of differences model for
565 both alignments. A maximum likelihood tree with 1000 bootstraps was produced in
566 RAxML 8.2.10 (Stamatakis, 2014) using a Generalized Time-Reversible (GTR)+G
567 model for both B19V and HBV.
568 To test the presence of a temporal structure in our DS2 (HBV and B19V) a root-tip
569 distance analysis was performed on Tempest 1.5.3 (Rambaut et al., 2016), a more
570 detailed analysis was also carried out on a subset (HBV/DS2.1) of sequences just
571 containing genomes from the HBV Genotype A.

572 The temporal structure found in the B19V/DS2 with the root-tip distance analysis
573 was corroborated by a date randomization test (DRT) using 20 combinations of our
574 B19V/DS2 with TipDatingBeast 1.0.5 (Rieux & Khatchikian, 2017) and BEAST 2.5.1
575 (Drummond et al., 2012).
576 Since our B19V/DS2 presented a clock-like structure with both methods, a dated
577 Bayesian analysis was generated to estimate the impact of the Colonial viral
578 genomes on the divergence time from the most recent common ancestor (MRCA).
579 We used BEAST 2.5.1 (Drummond et al., 2012), with a relaxed lognormal or strict
580 molecular clock with constant population, Bayesian skyline population or coalescent
581 exponential population prior. All parameters were mixed and converged into an
582 estimated sample size (ESS) >200 analyzed in Tracer 1.7 (Rambaut et al., 2018).
583 The first 25% of trees where discarded (burn in) and a Maximum Clade Credibility
584 Tree was created with TreeAnnotator (Drummond et al., 2012). The generated trees
585 were visualized and edited in FigTree 1.4.3 with a midpoint root.
586
587 *Human population genetic analyses*
588 Human-mapped reads (BWA aln) obtained from the pre-capture sequence data of
589 viral-positive samples were used to infer the genetic ancestry of the hosts. A
590 Principal Components Analysis (PCA) was carried out using 10 populations (IBS:
591 Iberian from Spain; CEU: Utah Residents with Northern and Western European
592 Ancestry ; CHB: Han Chinese in Beijing; MXL: Mexican Ancestry from Los Angeles;
593 PEL: Peruvians from Lima; CHS: Southern Han Chinese; YRI: Yoruba in Ibadan;
594 ESN: Esan in Nigeria; GWD: Gambian; MSL: Mende in Sierra Leone) from the 1000
595 Genomes Project (1000 Genomes Project Consortium et al., 2015) reference panel

including genotype data of 1,562,771 single nucleotide variants (SNVs) present in the MEGA array (Wojcik et al., 2019) from 2,504 individuals (phase 3). Genomic alignments of each ancient individual (HSJNC81, HSJN240, HSJN194 and COYC4) were intersected with the positions of the SNVs present in the reference panel genotype data. Pseudo haploid genotypes were called by randomly selecting one allele at each intersected site and filtering by a base quality >30. Pseudo haploid genotypes were also called for the complete reference panel. PCA was performed on the merged ancient and modern dataset with smartpca (EIGENSOFT package) (Patterson et al., 2006; A. L. Price et al., 2006) using the option *lsqproject* to project the ancient individuals into the PC space defined by the modern individuals.

Ancestry composition of individual COYC4

A total of 1,246 sites intersected between the 1000 Genomes Project reference panel and COYC4 ancient genome (see previous section for details). The program ADMIXTURE (Alexander & Lange, 2011) was run with K values of 2 to 5 and 100 replicates for each K using a different seed number. For each K, the ADMIXTURE run with the best likelihood was chosen to plot it using AncestryPainter (Feng et al., 2018).

Mitochondrial haplogroup and sex determination

NGS reads were mapped to the human mitochondrial genome reference (rCRS) with BWA (aln algorithm, -l default), the alignment file was then used to generate a consensus mitochondrial genome with the program Schmutzi(Renaud et al., 2015) The assignment of the mitochondrial haplogroup was carried out with Haplogrep

620 (Kloss-Brandstätter et al., 2011; Weissensteiner et al., 2016) using the consensus
621 sequence as the input. Assignment of biological sex was inferred based on the
622 fraction of reads mapped to the Y-chromosome (Ry) compared to those mapping to
623 the Y and X-chromosome (Skoglund et al., 2013). Ry<0.016 and Ry>0.075 were
624 considered XX or XY genotype, respectively. The resulting sex was coherent with
625 the one inferred morphologically (Supplementary Methods).
626

627 **ACKNOWLEDGMENTS**

628 This work was funded by the Wellcome Trust Sanger grant number 208934/Z/17/Z,
629 and by project IA201219 PAPIIT-DGAPA-UNAM. D.B-M is an Open Philanthropy
630 Fellow of the Life Sciences Research Foundation (LSRF). We thank the INAH
631 Archeology Council for the sample permissions 401.1S.3-2018/1373 and 401.1S.3-
632 2020/1310 for this study using samples from the Hospital San Jose de los Naturales
633 and the Temple of Immaculate Conception (La Conchita), respectively. We are
634 grateful with Teodoro Hernández Treviño, Gerardo Arrieta García from the
635 “Laboratorio Universitario de Geoquímica Isotópica” (LUGIS-UNAM) for their
636 technical support in performing the $^{87}Sr/^{86}Sr$ analyses and to Luis Alberto Aguilar
637 Bautista, Alejandro de León Cuevas, Carlos Sair Flores Bautista and Jair Garcia
638 Sotelo from the “Laboratorio Nacional de Visualización Científica Avanzada”
639 (LAVIS/UNAM) who stored our data and provided the computational resources to
640 perform this study. We thank Alejandra Castillo Carbajal and Carina Uribe Díaz for
641 technical support throughout the project.
642

643 **DATA AVAILABILITY**

644 Reconstructed genomes from this study are available in Genbank under accession
645 number MT108214, MT108215, MT108216, MT108217. Accession number of
646 sequences used in phylogenetic analysis are indicated in supplementary
647 information. NGS data is available upon reasonable request.

REFERENCES:

1000 Genomes Project Consortium, Auton, A., Brooks, L. D., Durbin, R. M., Garrison, E. P., Kang, H. M., Korbel, J. O., Marchini, J. L., McCarthy, S., McVean, G. A., & Abecasis, G. R. (2015). A global reference for human genetic variation. *Nature*, *526*(7571), 68–74. https://doi.org/10.1038/nature15393

Acuña-Soto, R., Stahle, D. W., Cleaveland, M. K., & Therrell, M. D. (2002). Megadrought and Megadeath in 16th Century Mexico. *Emerging Infectious Diseases*, *8*(4), 360–362. https://doi.org/10.3201/eid0804.010175

Acuña-Soto, R., Stahle, D. W., Therrell, M. D., Griffin, R. D., & Cleaveland, M. K. (2004). When half of the population died: The epidemic of hemorrhagic fevers of 1576 in Mexico. *FEMS Microbiology Letters*, *240*(1), 1–5. https://doi.org/10.1016/j.femsle.2004.09.011

Aguirre-Beltrán, G. (2005). La presencia del negro en México. *Revista Del CESLA*, *7*, 351–367.

Alexander, D. H., & Lange, K. (2011). Enhancements to the ADMIXTURE algorithm for individual ancestry estimation. *BMC Bioinformatics*, *12*, 246. https://doi.org/10.1186/1471-2105-12-246

Altschul, S. F., Gish, W., Miller, W., Myers, E. W., & Lipman, D. J. (1990). Basic local alignment search tool. *Journal of Molecular Biology*, *215*(3), 403–410. https://doi.org/10.1016/S0022-2836(05)80360-2

Alvarado-Mora, M. V., Romano, C. M., Gomes-Gouvêa, M. S., Gutierrez, M. F., Carrilho, F. J., & Pinho, J. R. R. (2012). Phylogenetic analysis of complete genome sequences of hepatitis B virus from an Afro-Colombian community: Presence of HBV F3/A1 recombinant strain. *Virology Journal*, *9*, 244.

https://doi.org/10.1186/1743-422X-9-244

Andernach, I. E., Nolte, C., Pape, J. W., & Muller, C. P. (2009). Slave trade and hepatitis B virus genotypes and subgenotypes in Haiti and Africa. *Emerging Infectious Diseases*, *15*(8), 1222–1228. https://doi.org/10.3201/eid1508.081642

Angel, J. L. (1966). Porotic hyperostosis, anemias, malarias, and marshes in the prehistoric Eastern Mediterranean. *Science (New York, N.Y.)*, *153*(3737), 760–763. https://doi.org/10.1126/science.153.3737.760

Barquera, R., Lamnidis, T. C., Lankapalli, A. K., Kocher, A., Hernández-Zaragoza, D. I., Nelson, E. A., Zamora-Herrera, A. C., Ramallo, P., Bernal-Felipe, N., Immel, A., Bos, K., Acuña-Alonzo, V., Barbieri, C., Roberts, P., Herbig, A., Kühnert, D., Márquez-Morfín, L., & Krause, J. (2020). Origin and Health Status of First-Generation Africans from Early Colonial Mexico. *Current Biology*, S0960982220304826. https://doi.org/10.1016/j.cub.2020.04.002

Bastos, M. Q. R., Santos, R. V., M. de Souza, S. M. F., Rodrigues-Carvalho, C., Tykot, R. H., Cook, D. C., & Santos, R. V. (2016). Isotopic study of geographic origins and diet of enslaved Africans buried in two Brazilian cemeteries. *Journal of Archaeological Science*, *70*, 82–90. https://doi.org/10.1016/j.jas.2016.04.020

Brichler, S., Lagathu, G., Chekaraou, M. A., Le Gal, F., Edouard, A., Dény, P., Césaire, R., & Gordien, E. (2013). African, Amerindian and European hepatitis B virus strains circulate on the Caribbean Island of Martinique. *The Journal of General Virology*, *94*(Pt 10), 2318–2329. https://doi.org/10.1099/vir.0.055459-0

Briggs, A. W., Stenzel, U., Johnson, P. L. F., Green, R. E., Kelso, J., Prüfer, K., Meyer, M., Krause, J., Ronan, M. T., Lachmann, M., & Pääbo, S. (2007). Patterns of damage in genomic DNA sequences from a Neandertal. *Proceedings of the*

696 *National Academy of Sciences of the United States of America*, *104*(37), 14616–
697 14621. https://doi.org/10.1073/pnas.0704665104
698 Broliden, K., Tolfvenstam, T., & Norbeck, O. (2006). Clinical aspects of parvovirus
699 B19 infection. *Journal of Internal Medicine*, *260*(4), 285–304.
700 https://doi.org/10.1111/j.1365-2796.2006.01697.x
701 Bryant, J. E., Holmes, E. C., & Barrett, A. D. T. (2007). Out of Africa: A Molecular
702 Perspective on the Introduction of Yellow Fever Virus into the Americas. *PLoS*
703 *Pathogens*, *3*(5). https://doi.org/10.1371/journal.ppat.0030075
704 Candotti, D., Etiz, N., Parsyan, A., & Allain, J.-P. (2004). Identification and
705 Characterization of Persistent Human Erythrovirus Infection in Blood Donor
706 Samples. *Journal of Virology*, *78*(22), 12169–12178.
707 https://doi.org/10.1128/JVI.78.22.12169-12178.2004
708 Cheng, A. P., Burnham, P., Lee, J. R., Cheng, M. P., Suthanthiran, M., Dadhania,
709 D., & De Vlaminck, I. (2019). A cell-free DNA metagenomic sequencing assay that
710 integrates the host injury response to infection. *Proceedings of the National*
711 *Academy of Sciences*, *116*(37), 18738–18744.
712 https://doi.org/10.1073/pnas.1906320116
713 Dabney, J., Knapp, M., Glocke, I., Gansauge, M.-T., Weihmann, A., Nickel, B.,
714 Valdiosera, C., García, N., Pääbo, S., Arsuaga, J.-L., & Meyer, M. (2013).
715 Complete mitochondrial genome sequence of a Middle Pleistocene cave bear
716 reconstructed from ultrashort DNA fragments. *Proceedings of the National*
717 *Academy of Sciences of the United States of America*, *110*(39), 15758–15763.
718 https://doi.org/10.1073/pnas.1314445110
719 Darriba, D., Taboada, G. L., Doallo, R., & Posada, D. (2012). jModelTest 2: More

models, new heuristics and high-performance computing. *Nature Methods*, *9*(8), 772. https://doi.org/10.1038/nmeth.2109

De Los Ángeles Ribas, M., Tejero, Y., Cordero, Y., Pérez, D., Sausy, A., Muller, C. P., & Hübschen, J. M. (2019). Identification of human parvovirus B19 among measles and rubella suspected patients from Cuba. *Journal of Medical Virology*, *91*(7), 1351–1354. https://doi.org/10.1002/jmv.25444

Drummond, A. J., Suchard, M. A., Xie, D., & Rambaut, A. (2012). Bayesian Phylogenetics with BEAUti and the BEAST 1.7. *Molecular Biology and Evolution*, *29*(8), 1969–1973. https://doi.org/10.1093/molbev/mss075

Duggan, A. T., Perdomo, M. F., Piombino-Mascali, D., Marciniak, S., Poinar, D., Emery, M. V., Buchmann, J. P., Duchêne, S., Jankauskas, R., Humphreys, M., Golding, G. B., Southon, J., Devault, A., Rouillard, J.-M., Sahl, J. W., Dutour, O., Hedman, K., Sajantila, A., Smith, G. L., … Poinar, H. N. (2016). 17th Century Variola Virus Reveals the Recent History of Smallpox. *Current Biology: CB*, *26*(24), 3407–3412. https://doi.org/10.1016/j.cub.2016.10.061

Düx, A., Lequime, S., Patrono, L. V., Vrancken, B., Boral, S., Gogarten, J. F., Hilbig, A., Horst, D., Merkel, K., Prepoint, B., Santibanez, S., Schlotterbeck, J., Suchard, M. A., Ulrich, M., Widulin, N., Mankertz, A., Leendertz, F. H., Harper, K., Schnalke, T., … Calvignac-Spencer, S. (2020). Measles virus and rinderpest virus divergence dated to the sixth century BCE. *Science*, *368*(6497), 1367–1370. https://doi.org/10.1126/science.aba9411

Feng, Q., Lu, D., & Xu, S. (2018). AncestryPainter: A Graphic Program for Displaying Ancestry Composition of Populations and Individuals. *Genomics, Proteomics & Bioinformatics*, *16*(5), 382–385.

744 https://doi.org/10.1016/j.gpb.2018.05.002

745 Forni, D., Pontremoli, C., Clerici, M., Pozzoli, U., Cagliani, R., & Sironi, M. (2020).

746 Recent out-of-Africa migration of human herpes simplex viruses. *Molecular Biology*

747 *and Evolution*, msaa001. https://doi.org/10.1093/molbev/msaa001

748 Freitas, R. B., Melo, F. L., Oliveira, D. S., Romano, C. M., Freitas, M. R. C.,

749 Macêdo, O., Linhares, A. C., de A Zanotto, P. M., & Durigon, E. L. (2008).

750 Molecular characterization of human erythrovirus B19 strains obtained from

751 patients with several clinical presentations in the Amazon region of Brazil. *Journal*

752 *of Clinical Virology: The Official Publication of the Pan American Society for*

753 *Clinical Virology*, *43*(1), 60–65. https://doi.org/10.1016/j.jcv.2008.03.033

754 Fricke, F., Laffoon, J., Victorina, A., & Haviser, J. (2020). Delayed physical

755 development in a first generation enslaved African woman from Pietermaai,

756 Curaçao. *International Journal of Osteoarchaeology*, *30*(1), 43–52.

757 https://doi.org/10.1002/oa.2829

758 Gadelha, S. R., Aleluia, M. M., Mello, M. A., Rego, F. F., Pereira, L. S., Galvão-

759 Castro, B., Gonçalves, M., Sousa, S. M., & Alcântara, L. C. (2014). The origin of

760 HTLV-1 in the South Bahia by phylogenetic, mitochondrial DNA and β-globin

761 analysis. *Retrovirology*, *11*(Suppl 1), P49. https://doi.org/10.1186/1742-4690-11-

762 S1-P49

763 Heegaard, E. D., & Brown, K. E. (2002). Human Parvovirus B19. *Clinical*

764 *Microbiology Reviews*, *15*(3), 485–505. https://doi.org/10.1128/CMR.15.3.485-

765 505.2002

766 Hernández-Lopez, P. E., & Negrete, S. (2012). *¿Realmente Eran Indios? Afinidad*

767 *biológica entre las personas atendidas en el Hospital Real San Jose de los*

Naturales, siglos XVI - XVIII. Escuela Nacional de Antropología e Historia.

Hübschen, J. M., Mihneva, Z., Mentis, A. F., Schneider, F., Aboudy, Y., Grossman, Z., Rudich, H., Kasymbekova, K., Sarv, I., Nedeljkovic, J., Tahita, M. C., Tarnagda, Z., Ouedraogo, J.-B., Gerasimova, A. G., Moskaleva, T. N., Tikhonova, N. T., Chitadze, N., Forbi, J. C., Faneye, A. O., … Muller, C. P. (2009). Phylogenetic analysis of human parvovirus b19 sequences from eleven different countries confirms the predominance of genotype 1 and suggests the spread of genotype 3b. *Journal of Clinical Microbiology*, *47*(11), 3735–3738. https://doi.org/10.1128/JCM.01201-09

Huson, D. H., Beier, S., Flade, I., Górska, A., El-Hadidi, M., Mitra, S., Ruscheweyh, H.-J., & Tappu, R. (2016). MEGAN Community Edition—Interactive Exploration and Analysis of Large-Scale Microbiome Sequencing Data. *PLoS Computational Biology*, *12*(6), e1004957. https://doi.org/10.1371/journal.pcbi.1004957

Jain, P., Jain, A., Prakash, S., Khan, D. N., Singh, D. D., Kumar, A., Moulik, N. R., & Chandra, T. (2015). Prevalence and genotypic characterization of human parvovirus B19 in children with hemato-oncological disorders in North India. *Journal of Medical Virology*, *87*(2), 303–309. https://doi.org/10.1002/jmv.24028

Jónsson, H., Ginolhac, A., Schubert, M., Johnson, P. L. F., & Orlando, L. (2013). mapDamage2.0: Fast approximate Bayesian estimates of ancient DNA damage parameters. *Bioinformatics (Oxford, England)*, *29*(13), 1682–1684. https://doi.org/10.1093/bioinformatics/btt193

Kahila Bar-Gal, G., Kim, M. J., Klein, A., Shin, D. H., Oh, C. S., Kim, J. W., Kim, T.-H., Kim, S. B., Grant, P. R., Pappo, O., Spigelman, M., & Shouval, D. (2012). Tracing hepatitis B virus to the 16th century in a Korean mummy. *Hepatology*,

56(5), 1671–1680. https://doi.org/10.1002/hep.25852

Karam-Tapia, C. E. (2012). *Estimación del Mestizaje Mediante la Morfología Dental en la Ciudad de México (Siglo XVI al XIX)*. Escuela Nacional de Antropología e Historia.

Kearse, M., Moir, R., Wilson, A., Stones-Havas, S., Cheung, M., Sturrock, S., Buxton, S., Cooper, A., Markowitz, S., Duran, C., Thierer, T., Ashton, B., Meintjes, P., & Drummond, A. (2012). Geneious Basic: An integrated and extendable desktop software platform for the organization and analysis of sequence data. *Bioinformatics*, *28*(12), 1647–1649. https://doi.org/10.1093/bioinformatics/bts199

Key, F. M., Posth, C., Krause, J., Herbig, A., & Bos, K. I. (2017). Mining Metagenomic Data Sets for Ancient DNA: Recommended Protocols for Authentication. *Trends in Genetics: TIG*, *33*(8), 508–520. https://doi.org/10.1016/j.tig.2017.05.005

Kloss-Brandstätter, A., Pacher, D., Schönherr, S., Weissensteiner, H., Binna, R., Specht, G., & Kronenberg, F. (2011). HaploGrep: A fast and reliable algorithm for automatic classification of mitochondrial DNA haplogroups. *Human Mutation*, *32*(1), 25–32. https://doi.org/10.1002/humu.21382

Kostaki, E.-G., Karamitros, T., Stefanou, G., Mamais, I., Angelis, K., Hatzakis, A., Kramvis, A., & Paraskevis, D. (2018). Unravelling the history of hepatitis B virus genotypes A and D infection using a full-genome phylogenetic and phylogeographic approach. *ELife*, *7*. https://doi.org/10.7554/eLife.36709

Kramvis, A. (2014). Genotypes and Genetic Variability of Hepatitis B Virus. *Intervirology*, *57*(3–4), 141–150. https://doi.org/10.1159/000360947

Krause-Kyora, B., Susat, J., Key, F. M., Kühnert, D., Bosse, E., Immel, A., Rinne,

C., Kornell, S.-C., Yepes, D., Franzenburg, S., Heyne, H. O., Meier, T., Lösch, S., Meller, H., Friederich, S., Nicklisch, N., Alt, K. W., Schreiber, S., Tholey, A., … Krause, J. (2018). Neolithic and medieval virus genomes reveal complex evolution of hepatitis B. *ELife*, *7*. https://doi.org/10.7554/eLife.36666

Kumar, S., Stecher, G., Li, M., Knyaz, C., & Tamura, K. (2018). MEGA X: Molecular Evolutionary Genetics Analysis across Computing Platforms. *Molecular Biology and Evolution*, *35*(6), 1547–1549. https://doi.org/10.1093/molbev/msy096

Larsson, A. (2014). AliView: A fast and lightweight alignment viewer and editor for large datasets. *Bioinformatics*, *30*(22), 3276–3278. https://doi.org/10.1093/bioinformatics/btu531

Li, H., Handsaker, B., Wysoker, A., Fennell, T., Ruan, J., Homer, N., Marth, G., Abecasis, G., Durbin, R., & 1000 Genome Project Data Processing Subgroup. (2009). The Sequence Alignment/Map format and SAMtools. *Bioinformatics*, *25*(16), 2078–2079. https://doi.org/10.1093/bioinformatics/btp352

Li, Heng, & Durbin, R. (2009). Fast and accurate short read alignment with Burrows–Wheeler transform. *Bioinformatics*, *25*(14), 1754–1760. https://doi.org/10.1093/bioinformatics/btp324

Lindahl, T. (1993). Instability and decay of the primary structure of DNA. *Nature*, *362*(6422), 709–715. https://doi.org/10.1038/362709a0

Lindo, J., Huerta-Sánchez, E., Nakagome, S., Rasmussen, M., Petzelt, B., Mitchell, J., Cybulski, J. S., Willerslev, E., DeGiorgio, M., & Malhi, R. S. (2016). A time transect of exomes from a Native American population before and after European contact. *Nature Communications*, *7*(1), 13175. https://doi.org/10.1038/ncomms13175

840 Luo, Y., & Qiu, J. (2015). Human parvovirus B19: A mechanistic overview of
841 infection and DNA replication. *Future Virology*, *10*(2), 155–167.
842 https://doi.org/10.2217/fvl.14.103
843 Malvido, E., & Viesca, C. (1982). La epidemia de cocoliztli de 1576. In E.
844 Florescano & E. Malvido (Eds.), *Ensayos sobre la historia de las epidemias en*
845 *México.* (pp. 27–32). Instituto Mexicano del Seguro Social.
846 Mandujano-Sánchez, A., Solache, L. C., & Mandujano, M. A. (1982). Historia de
847 las Epidemias en el México Antiguo: Algunos Aspectos Biológicos y Sociales. In E.
848 Florescano & E. Malvido (Eds.), *Ensayos sobre la historia de las epidemias en*
849 *México.* (pp. 9–21). Instituto Mexicano del Seguro Social.
850 Markov, P. V., Pepin, J., Frost, E., Deslandes, S., Labbé, A.-C., & Pybus, O. G.
851 (2009). Phylogeography and molecular epidemiology of hepatitis C virus genotype
852 2 in Africa. *The Journal of General Virology*, *90*(Pt 9), 2086–2096.
853 https://doi.org/10.1099/vir.0.011569-0
854 Marr, J. S., & Kiracofe, J. B. (2000). Was the huey cocoliztli a haemorrhagic fever?
855 *Medical History*, *44*(3), 341–362.
856 Meyer, M., & Kircher, M. (2010). Illumina Sequencing Library Preparation for Highly
857 Multiplexed Target Capture and Sequencing. *Cold Spring Harbor Protocols*,
858 *2010*(6), 1–10. https://doi.org/10.1101/pdb.prot5448
859 Meza, A. (2013). Presencia africana en el cementerio del Hospital Real de San
860 Jóse de los Naturales. *Arqueología mexicana*, *119*, 40–44.
861 Moreno-Cabrera, M. de la L., Meraz-Moreno, A., & Cervantes-Rosado, J. (2015).
862 Relleno aligerado con vasijas cerámicas en el templo de la Inmaculada
863 Concepción, en Coyoacán. In *Boletín de monumentos históricos 35* (Vol. 35, pp.

121–134). Instituto Nacional de Antropología e Historia.

Mühlemann, B., Jones, T. C., Damgaard, P. de B., Allentoft, M. E., Shevnina, I., Logvin, A., Usmanova, E., Panyushkina, I. P., Boldgiv, B., Bazartseren, T., Tashbaeva, K., Merz, V., Lau, N., Smrčka, V., Voyakin, D., Kitov, E., Epimakhov, A., Pokutta, D., Vicze, M., … Willerslev, E. (2018). Ancient hepatitis B viruses from the Bronze Age to the Medieval period. *Nature*, *557*(7705), 418–423. https://doi.org/10.1038/s41586-018-0097-z

Mühlemann, B., Margaryan, A., Damgaard, P. de B., Allentoft, M. E., Vinner, L., Hansen, A. J., Weber, A., Bazaliiskii, V. I., Molak, M., Arneborg, J., Bogdanowicz, W., Falys, C., Sablin, M., Smrčka, V., Sten, S., Tashbaeva, K., Lynnerup, N., Sikora, M., Smith, D. J., … Jones, T. C. (2018). Ancient human parvovirus B19 in Eurasia reveals its long-term association with humans. *Proceedings of the National Academy of Sciences of the United States of America*, *115*(29), 7557–7562. https://doi.org/10.1073/pnas.1804921115

Mühlemann, B., Vinner, L., Margaryan, A., Wilhelmson, H., de la Fuente Castro, C., Allentoft, M. E., de Barros Damgaard, P., Hansen, A. J., Holtsmark Nielsen, S., Strand, L. M., Bill, J., Buzhilova, A., Pushkina, T., Falys, C., Khartanovich, V., Moiseyev, V., Jørkov, M. L. S., Østergaard Sørensen, P., Magnusson, Y., … Sikora, M. (2020). Diverse variola virus (smallpox) strains were widespread in northern Europe in the Viking Age. *Science (New York, N.Y.)*, *369*(6502). https://doi.org/10.1126/science.aaw8977

Neukamm, J., Pfrengle, S., Molak, M., Seitz, A., Francken, M., Eppenberger, P., Avanzi, C., Reiter, E., Urban, C., Welte, B., Stockhammer, P. W., Teßmann, B., Herbig, A., Harvati, K., Nieselt, K., Krause, J., & Schuenemann, V. J. (2020). 2000-

888 year-old pathogen genomes reconstructed from metagenomic analysis of Egyptian
889 mummified individuals. *BMC Biology*, *18*(1), 108. https://doi.org/10.1186/s12915-
890 020-00839-8
891 Nguyen, Q. T., Sifer, C., Schneider, V., Allaume, X., Servant, A., Bernaudin, F.,
892 Auguste, V., & Garbarg-Chenon, A. (1999). Novel Human Erythrovirus Associated
893 with Transient Aplastic Anemia. *Journal of Clinical Microbiology*, *37*(8), 2483–2487.
894 Ondov, B. D., Bergman, N. H., & Phillippy, A. M. (2011). Interactive metagenomic
895 visualization in a Web browser. *BMC Bioinformatics*, *12*(1), 385.
896 https://doi.org/10.1186/1471-2105-12-385
897 Pajer, P., Dresler, J., Kabíckova, H., Písa, L., Aganov, P., Fucik, K., Elleder, D.,
898 Hron, T., Kuzelka, V., Velemínsky, P., Klimentova, J., Fucikova, A., Pejchal, J.,
899 Hrabakova, R., Benes, V., Rausch, T., Dundr, P., Pilin, A., Cabala, R., … Meyer,
900 H. (2017). Characterization of Two Historic Smallpox Specimens from a Czech
901 Museum. *Viruses*, *9*(8). https://doi.org/10.3390/v9080200
902 Patterson, N., Price, A. L., & Reich, D. (2006). Population Structure and
903 Eigenanalysis. *PLoS Genetics*, *2*(12), e190.
904 https://doi.org/10.1371/journal.pgen.0020190
905 Patterson Ross, Z., Klunk, J., Fornaciari, G., Giuffra, V., Duchêne, S., Duggan, A.
906 T., Poinar, D., Douglas, M. W., Eden, J.-S., Holmes, E. C., & Poinar, H. N. (2018).
907 The paradox of HBV evolution as revealed from a 16th century mummy. *PLoS*
908 *Pathogens*, *14*(1), e1006750. https://doi.org/10.1371/journal.ppat.1006750
909 Pourkarim, M. R., Amini-Bavil-Olyaee, S., Kurbanov, F., Van Ranst, M., & Tacke,
910 F. (2014). Molecular identification of hepatitis B virus genotypes/subgenotypes:
911 Revised classification hurdles and updated resolutions. *World Journal of*

912 *Gastroenterology*, *20*(23), 7152–7168. https://doi.org/10.3748/wjg.v20.i23.7152

913 Pourkarim, M. R., Lemey, P., Amini-Bavil-Olyaee, S., Maes, P., & Van Ranst, M.

914 (2010). Novel hepatitis B virus subgenotype A6 in African-Belgian patients. *Journal*

915 *of Clinical Virology: The Official Publication of the Pan American Society for*

916 *Clinical Virology*, *47*(1), 93–96. https://doi.org/10.1016/j.jcv.2009.09.032

917 Price, A. L., Patterson, N. J., Plenge, R. M., Weinblatt, M. E., Shadick, N. A., &

918 Reich, D. (2006). Principal components analysis corrects for stratification in

919 genome-wide association studies. *Nature Genetics*, *38*(8), 904–909.

920 https://doi.org/10.1038/ng1847

921 Price, T. D., Burton, J. H., Cucina, A., Zabala, P., Frei, R., Tykot, R. H., & Tiesler,

922 V. (2012). Isotopic Studies of Human Skeletal Remains from a Sixteenth to

923 Seventeenth Century AD Churchyard in Campeche, Mexico: Diet, Place of Origin,

924 and Age. *Current Anthropology*, *53*(4), 396–433. https://doi.org/10.1086/666492

925 Pruitt, K. D., Tatusova, T., & Maglott, D. R. (2007). NCBI reference sequences

926 (RefSeq): A curated non-redundant sequence database of genomes, transcripts

927 and proteins. *Nucleic Acids Research*, *35*(Database issue), D61-65.

928 https://doi.org/10.1093/nar/gkl842

929 Pyöriä, L., Toppinen, M., Mäntylä, E., Hedman, L., Aaltonen, L.-M., Vihinen-Ranta,

930 M., Ilmarinen, T., Söderlund-Venermo, M., Hedman, K., & Perdomo, M. F. (2017).

931 Extinct type of human parvovirus B19 persists in tonsillar B cells. *Nature*

932 *Communications*, *8*, 14930. https://doi.org/10.1038/ncomms14930

933 Quintero, A., Martínez, D., Alarcón De Noya, B., Costagliola, A., Urbina, L.,

934 González, N., Liprandi, F., Castro De Guerra, D., & Pujol, F. H. (2002). Molecular

935 epidemiology of hepatitis B virus in Afro-Venezuelan populations. *Archives of*

Virology, *147*(9), 1829–1836. https://doi.org/10.1007/s00705-002-0842-2

Rambaut, A., Drummond, A. J., Xie, D., Baele, G., & Suchard, M. A. (2018). Posterior Summarization in Bayesian Phylogenetics Using Tracer 1.7. *Systematic Biology*, *67*(5), 901–904. https://doi.org/10.1093/sysbio/syy032

Rambaut, A., Lam, T. T., Max Carvalho, L., & Pybus, O. G. (2016). Exploring the temporal structure of heterochronous sequences using TempEst (formerly Path-O-Gen). *Virus Evolution*, *2*(1), vew007. https://doi.org/10.1093/ve/vew007

Renaud, G., Slon, V., Duggan, A. T., & Kelso, J. (2015). Schmutzi: Estimation of contamination and endogenous mitochondrial consensus calling for ancient DNA. *Genome Biology*, *16*(1), 224. https://doi.org/10.1186/s13059-015-0776-0

Rezaei, F., Sarshari, B., Ghavami, N., Meysami, P., Shadab, A., Salimi, H., & Mokhtari-Azad, T. (2016). Prevalence and genotypic characterization of Human Parvovirus B19 in children with measles- and rubella-like illness in Iran. *Journal of Medical Virology*, *88*(6), 947–953. https://doi.org/10.1002/jmv.24425

Rieux, A., & Balloux, F. (2016). Inferences from tip-calibrated phylogenies: A review and a practical guide. *Molecular Ecology*, *25*(9), 1911–1924. https://doi.org/10.1111/mec.13586

Rieux, A., & Khatchikian, C. E. (2017). Tipdatingbeast an r package to assist the implementation of phylogenetic tip-dating tests using beast. *Molecular Ecology Resources*, *17*(4), 608–613. https://doi.org/10.1111/1755-0998.12603

Rinckel, L. A., Buno, B. R., Gierman, T. M., & Lee, D. C. (2009). Discovery and analysis of a novel parvovirus B19 Genotype 3 isolate in the United States. *Transfusion*, *49*(7), 1488–1492. https://doi.org/10.1111/j.1537-2995.2009.02160.x

Rohland, N., & Hofreiter, M. (2007). Ancient DNA extraction from bones and teeth.

Nature Protocols, *2*(7), 1756–1762. https://doi.org/10.1038/nprot.2007.247

Roman, S., Tanaka, Y., Khan, A., Kurbanov, F., Kato, H., Mizokami, M., & Panduro, A. (2010). Occult hepatitis B in the genotype H-infected Nahuas and Huichol native Mexican population. *Journal of Medical Virology*, *82*(9), 1527–1536. https://doi.org/10.1002/jmv.21846

Rotimi, C. N., Tekola-Ayele, F., Baker, J. L., & Shriner, D. (2016). The African Diaspora: History, Adaptation and Health. *Current Opinion in Genetics & Development*, *41*, 77–84. https://doi.org/10.1016/j.gde.2016.08.005

Ruíz-Albarrán, P. (2012). *Estudio de variabilidad biológica en la colección esquelética Hospital Real de San José de los Naturales. Un acercamiento a tráves de la técnica de morfometría geométrica.* Escuela Nacional de Antropología e Historia.

Salas, A., Richards, M., Lareu, M.-V., Scozzari, R., Coppa, A., Torroni, A., Macaulay, V., & Carracedo, Á. (2004). The African Diaspora: Mitochondrial DNA and the Atlantic Slave Trade. *American Journal of Human Genetics*, *74*(3), 454–465.

Sanabani, S., Neto, W. K., Pereira, J., & Sabino, E. C. (2006). Sequence Variability of Human Erythroviruses Present in Bone Marrow of Brazilian Patients with Various Parvovirus B19-Related Hematological Symptoms. *Journal of Clinical Microbiology*, *44*(2), 604–606. https://doi.org/10.1128/JCM.44.2.604-606.2006

Schneider, B., Höne, A., Tolba, R. H., Fischer, H.-P., Blümel, J., & Eis-Hübinger, A. M. (2008). Simultaneous persistence of multiple genome variants of human parvovirus B19. *Journal of General Virology*, *89*(1), 164–176. https://doi.org/10.1099/vir.0.83053-0

Schroeder, H., O'Connell, T. C., Evans, J. A., Shuler, K. A., & Hedges, R. E. M. (2009). Trans-Atlantic slavery: Isotopic evidence for forced migration to Barbados. *American Journal of Physical Anthropology*, *139*(4), 547–557. https://doi.org/10.1002/ajpa.21019

Schubert, M., Ginolhac, A., Lindgreen, S., Thompson, J. F., Al-Rasheid, K. A. S., Willerslev, E., Krogh, A., & Orlando, L. (2012). Improving ancient DNA read mapping against modern reference genomes. *BMC Genomics*, *13*, 178. https://doi.org/10.1186/1471-2164-13-178

Schubert, M., Lindgreen, S., & Orlando, L. (2016). AdapterRemoval v2: Rapid adapter trimming, identification, and read merging. *BMC Research Notes*, *9*. https://doi.org/10.1186/s13104-016-1900-2

Servant, A., Laperche, S., Lallemand, F., Marinho, V., De Saint Maur, G., Meritet, J. F., & Garbarg-Chenon, A. (2002). Genetic Diversity within Human Erythroviruses: Identification of Three Genotypes. *Journal of Virology*, *76*(18), 9124–9134. https://doi.org/10.1128/JVI.76.18.9124-9134.2002

Skoglund, P., Storå, J., Götherström, A., & Jakobsson, M. (2013). Accurate sex identification of ancient human remains using DNA shotgun sequencing. *Journal of Archaeological Science*, *40*(12), 4477–4482. https://doi.org/10.1016/j.jas.2013.07.004

Somolinos d'Árdois, G. (1982). Las epidemias en México durante el siglo XVI. In E. Florescano & E. Malvido (Eds.), *Ensayos sobre la historia de las epidemias en México.* (pp. 138–143). Instituto Mexicano del Seguro Social.

Spyrou, M. A., Bos, K. I., Herbig, A., & Krause, J. (2019). Ancient pathogen genomics as an emerging tool for infectious disease research. *Nature Reviews.*

Genetics, *20*(6), 323–340. https://doi.org/10.1038/s41576-019-0119-1

Stamatakis, A. (2014). RAxML version 8: A tool for phylogenetic analysis and post-analysis of large phylogenies. *Bioinformatics*, *30*(9), 1312–1313. https://doi.org/10.1093/bioinformatics/btu033

Tithi, S. S., Aylward, F. O., Jensen, R. V., & Zhang, L. (2018). FastViromeExplorer: A pipeline for virus and phage identification and abundance profiling in metagenomics data. *PeerJ*, *6*, e4227. https://doi.org/10.7717/peerj.4227

Vågene, Å. J., Herbig, A., Campana, M. G., García, N. M. R., Warinner, C., Sabin, S., Spyrou, M. A., Valtueña, A. A., Huson, D., Tuross, N., Bos, K. I., & Krause, J. (2018). Salmonella enterica genomes from victims of a major sixteenth-century epidemic in Mexico. *Nature Ecology & Evolution*, *2*(3), 520. https://doi.org/10.1038/s41559-017-0446-6

Valencia Pacheco, G., Nakazawa Ueji, Y. E., Rodríguez Dzul, E. A., Angulo Ramírez, A. V., López Villanueva, R. F., Quintal Ortíz, I. G., & Rosado Paredes, E. P. (2017). Serological and molecular analysis of parvovirus B19 infection in Mayan women with systemic lupus erythematosus in Mexico. *Colombia Médica*, *v48*(i3), 105–112. https://doi.org/10.25100/cm.v48i3.2981

Warinner, C., Herbig, A., Mann, A., Fellows Yates, J. A., Weiß, C. L., Burbano, H. A., Orlando, L., & Krause, J. (2017). A Robust Framework for Microbial Archaeology. *Annual Review of Genomics and Human Genetics*, *18*, 321–356. https://doi.org/10.1146/annurev-genom-091416-035526

Weissensteiner, H., Pacher, D., Kloss-Brandstätter, A., Forer, L., Specht, G., Bandelt, H.-J., Kronenberg, F., Salas, A., & Schönherr, S. (2016). HaploGrep 2: Mitochondrial haplogroup classification in the era of high-throughput sequencing.

Nucleic Acids Research, *44*(W1), W58–W63. https://doi.org/10.1093/nar/gkw233

Wesp, J. K. (2017). Caring for Bodies or Simply Saving Souls: The Emergence of Institutional Care in Spanish Colonial America. In L. Tilley & A. A. Schrenk (Eds.), *New Developments in the Bioarchaeology of Care: Further Case Studies and Expanded Theory* (pp. 253–276). Springer International Publishing. https://doi.org/10.1007/978-3-319-39901-0_13

Wojcik, G. L., Graff, M., Nishimura, K. K., Tao, R., Haessler, J., Gignoux, C. R., Highland, H. M., Patel, Y. M., Sorokin, E. P., Avery, C. L., Belbin, G. M., Bien, S. A., Cheng, I., Cullina, S., Hodonsky, C. J., Hu, Y., Huckins, L. M., Jeff, J., Justice, A. E., … Carlson, C. S. (2019). Genetic analyses of diverse populations improves discovery for complex traits. *Nature*, *570*(7762), 514–518. https://doi.org/10.1038/s41586-019-1310-4

Xiao, Y.-L., Kash, J. C., Beres, S. B., Sheng, Z.-M., Musser, J. M., & Taubenberger, J. K. (2013). High-throughput RNA sequencing of a formalin-fixed, paraffin-embedded autopsy lung tissue sample from the 1918 influenza pandemic. *The Journal of Pathology*, *229*(4), 535–545. https://doi.org/10.1002/path.4145

Yuen, M.-F., Chen, D.-S., Dusheiko, G. M., Janssen, H. L. A., Lau, D. T. Y., Locarnini, S. A., Peters, M. G., & Lai, C.-L. (2018). Hepatitis B virus infection. *Nature Reviews. Disease Primers*, *4*, 18035. https://doi.org/10.1038/nrdp.2018.35

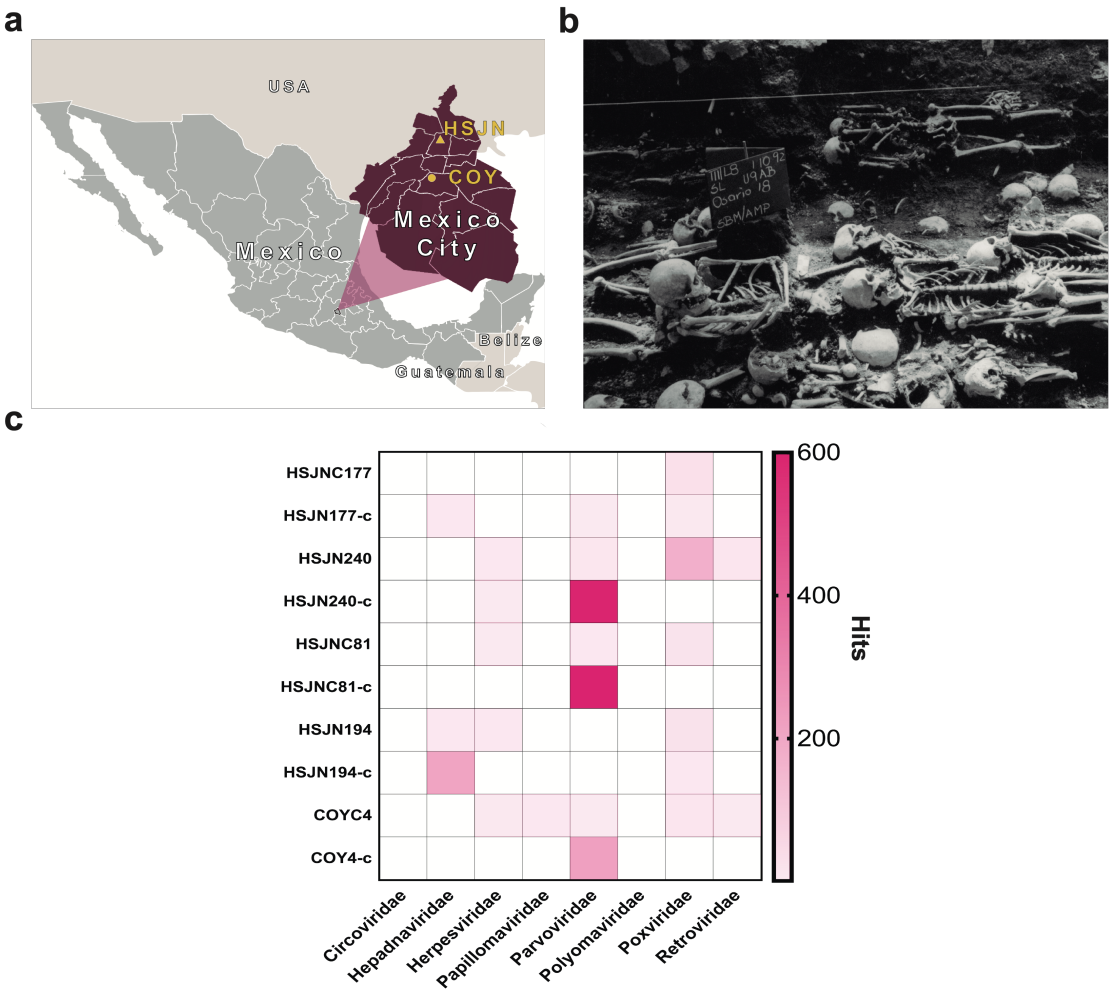

Figure 1. Metagenomic analysis of Colonial individuals reveal HBV-like and B19V-like hits. a) Location of the archeological sites used in this study, HSJN (19.431704, -99.141740) is shown as a yellow triangle and COY (19.347079, -99.159017) as a yellow circle, lines in pink map show current division of Mexico City. **b**) Several individuals discovered in massive burials archaeologically associated with the HSJN and colonial epidemics (photo courtesy of "Secretaria de Cultura INAH, SINAFO, Fototeca DSA"). **c**) Metagenomic analysis performed with MALT 0.4.0 based on the Viral NCBI RefSeq. Viral abundancies were compared and normalized automatically in MEGAN between shotgun (*sample_name*) and capture

(*sample_name*-c) NGS data. Only HBV or B19V positive samples are shown (all samples analyzed are shown in Supplementary Figure 2a-b). A capture negative control (HSJN177) is shown.

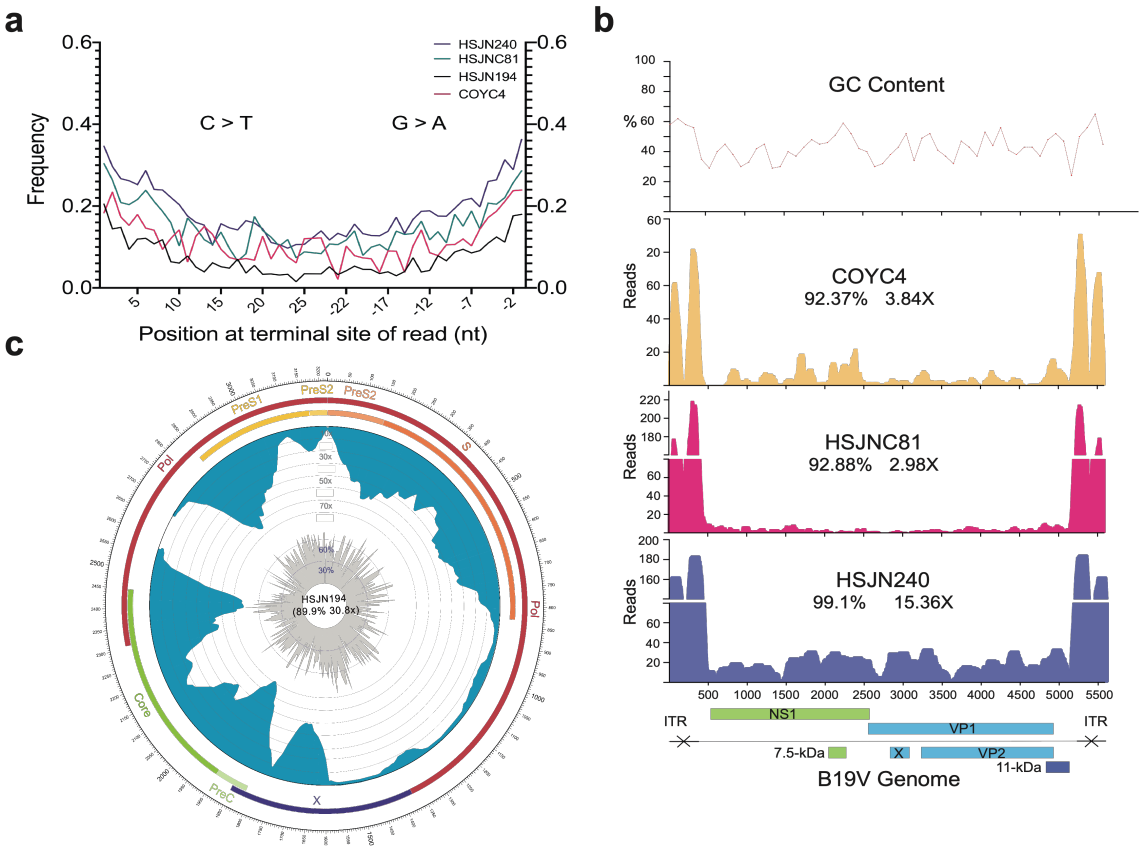

Figure 2. Ancient B19V and HBV ancient genomes. a) Superimposed damage patterns of ancient HBV (HSJN194) and B19V (HSJNC81, HSJN240, COYC4), X axis shows the position (nt) on the 5' (left) and 3' (right) end of the read, Y axis shows the damage frequency (raw individual damage patterns are shown on Supplementary Figure 3). **b**) B19V ssDNA linear genome, X axis shows position (nt) based on the reference genome (AB550331), and Y axis shows depth (as number of reads), GC content is shown as a percentage of each 100 bp windows, coverage and average depth for the CDS are shown under each individual ID. Schematic of the B19V genome is shown at the bottom. Highly covered regions correspond to dsDNA ITRs shown as crossed arrows. **c**) HBV circular genome, outer numbers show position (nt) based on reference genome (GQ331046), outer bars show genes

1079 with names, blue bars represent coverage and gray bars shows GC content each 10
1080 bp windows. Coverage and average depth are shown in the center. Low covered
1081 region between S and X overlaps with ssDNA region.
1082

1083

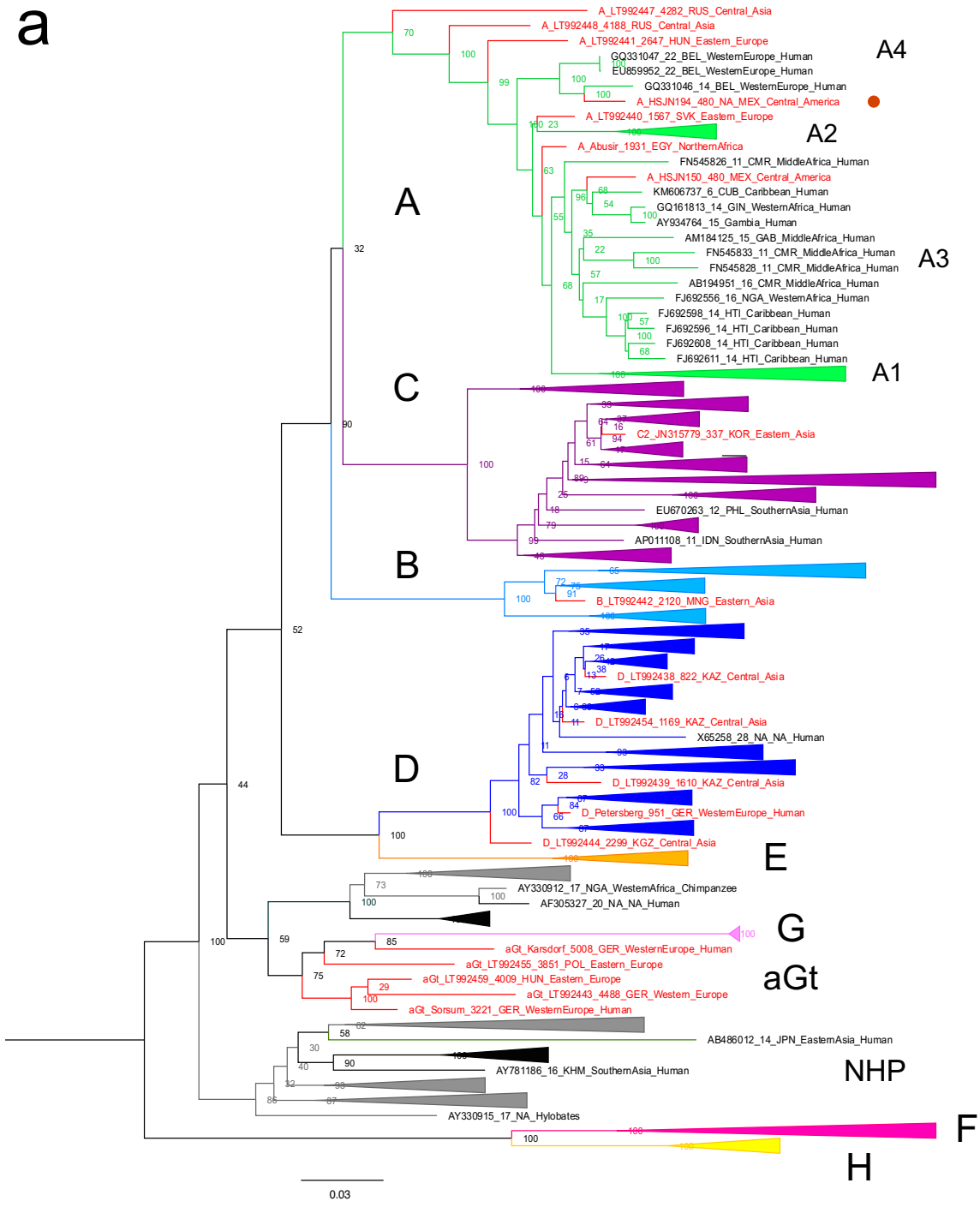

1084

1085

b

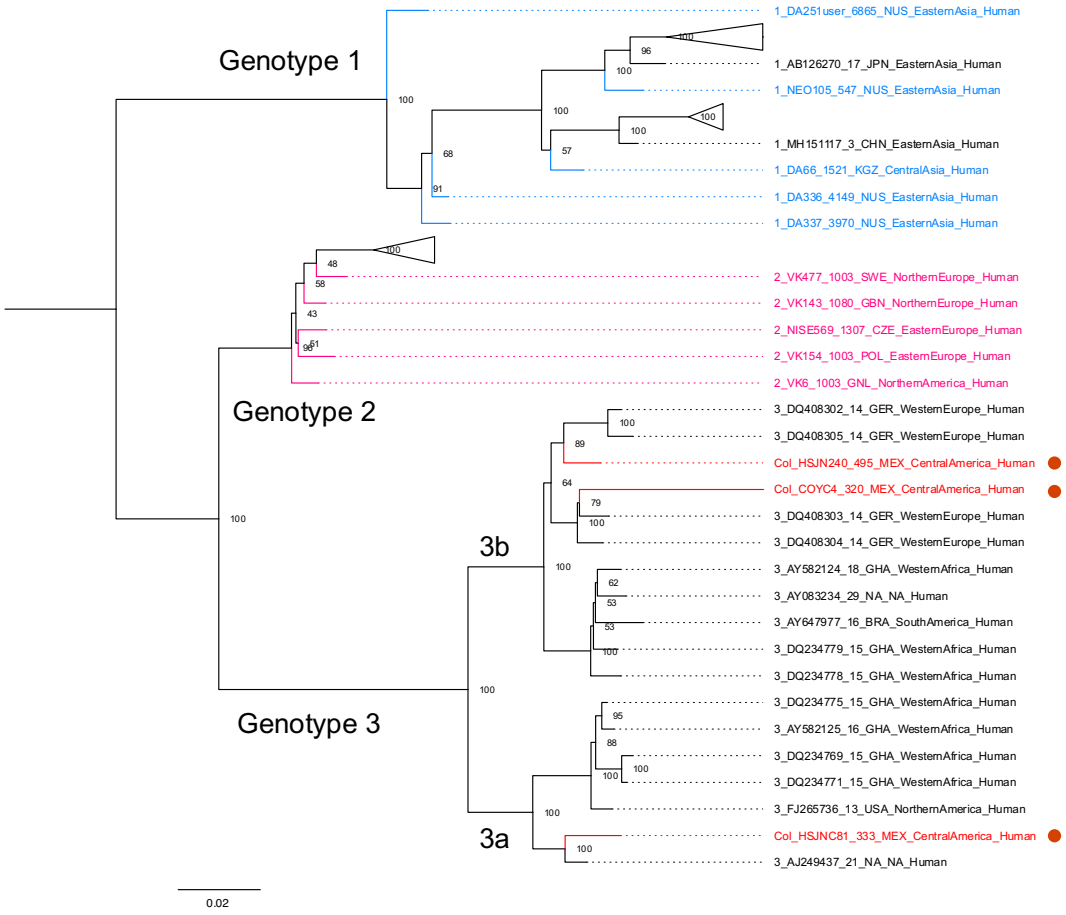

Figure 3. Viral Colonial genomes are similar to modern African genetic diversity. a-b. Maximum likelihood trees performed on RAxML 8.2.10 (1000 bootstraps) with a midpoint root, genotypes are named in bold letters and sub-genotypes in italics. Bootstrap values are shown at the node center and triangles represent collapsed sequences from other genotypes. Sequences are named as follows: genotype_ID_sampling.year_country.of.origin_area.of.origin_host. Sequences from this study are highlighted with a red circle on the right. **a)** Based on the HBV whole genome, genotypes are named with letters and each is colored

1095 differently, while ancient sequences are shown in red. NHP: non-human primates;

1096 **b)** based on B19V CDS where genotypes are named with numbers, and only ancient

1097 genomes are colored.

1098

a

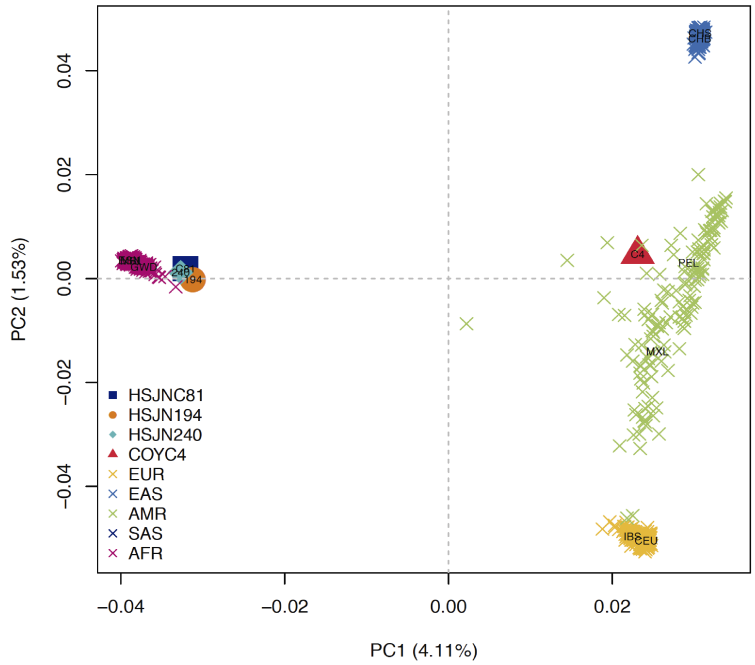

b

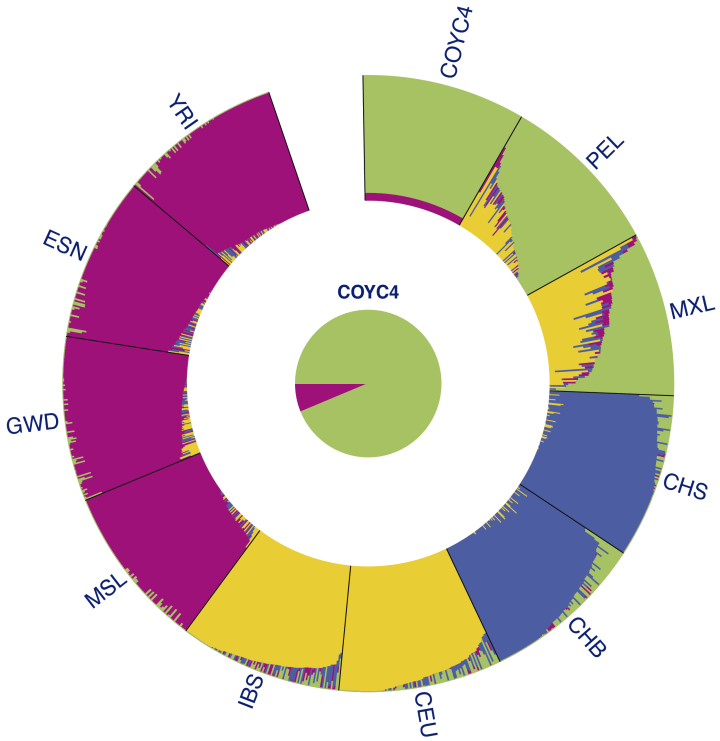

1099

Figure 4. Human hosts are similar to modern African genetic diversity. a) PCA showing genetic affinities of ancient human hosts compared to the 1000 Genomes Project reference panel. Crosses (X) show individuals from the reference panel while other shapes show human hosts from which ancient HBV (HSJN194) and B19V (HSJNC81, HSJN240, COYC4) sequences were recovered. Clusters are colored in five super populations EUR: Europeans (IBS, CEU); EAS: East Asian (CHB); AMR: Ad Mixed Americans (MXL, PEL); SAS: South Asians (CHS) and AFR: Africans (YRI, ESN, GWD, MSL). Three letter code is based on the 1000 Genomes Project nomenclature. **b)** Admixture analysis with COYC4 intersected sites with 1000 Genomes MEGA array, run with k=4 for 100 replicates. Each color shows a different component using the same colors as in the PCA. In the center a pie chart shows the proportion of native American (green) and African (magenta) genetic components.